

Supplementary material for:

Carbonate content and stable isotopic composition of aerosol carbon in the Canadian High Arctic

Petr Vodička^{1,2}, Kimitaka Kawamura², Bhagawati Kunwar^{2,3}, Lin Huang⁴, Dhananjay K. Deshmukh^{2,a}, Md. Mozammel Haque^{2,5}, Sangeeta Sharma⁴, Leonard Barrie⁶

¹ Institute of Chemical Process Fundamentals, Czech Academy of Sciences, 165 00 Prague 6, Czech Republic

² Chubu Institute for Advanced Studies, Chubu University, 1200 Matsumoto-cho, Kasugai 487–8501, Japan

³ Institute for Space-Earth Environmental Research, Nagoya University, Nagoya 464-8601, Japan

⁴ Environment and Climate Change Canada, Science and Technology Branch, 4905 Dufferin St., Toronto, Canada

⁵ School of Ecology and Applied Meteorology, NUIST, Nanjing, 210044, China

⁶ Atmospheric and Oceanic Sciences Department, McGill University, Montreal, Canada

^a Now at: Commission for Air Quality Management in National Capital Region and Adjoining Areas, New Delhi 110001, India

Correspondence to: Petr Vodička (vodicka@icpf.cas.cz) and Kimitaka Kawamura (kkawamura@isc.chubu.ac.jp)

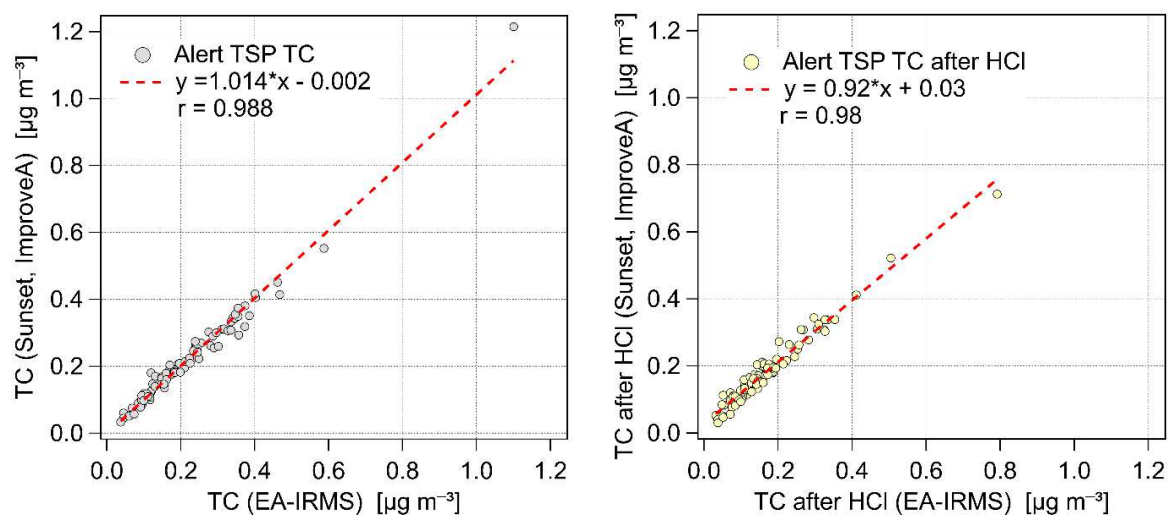


Figure S1. Comparison of TC concentrations measured by the EA and by the EC/OC analyzer on the same filters before any treatment (left) and after HCl fumigation (right).

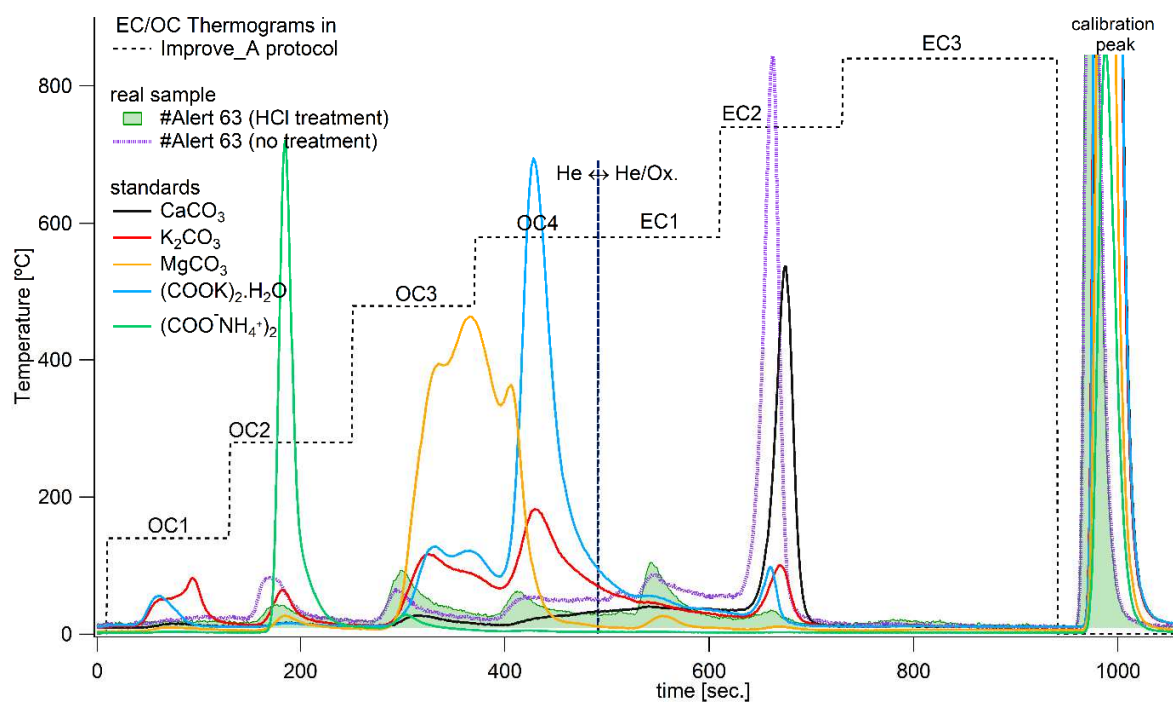


Figure S2. EC/OC thermograms of one Alert sample (#63) before and after HCl treatment together with thermograms of carbonate and oxalate salts standards.

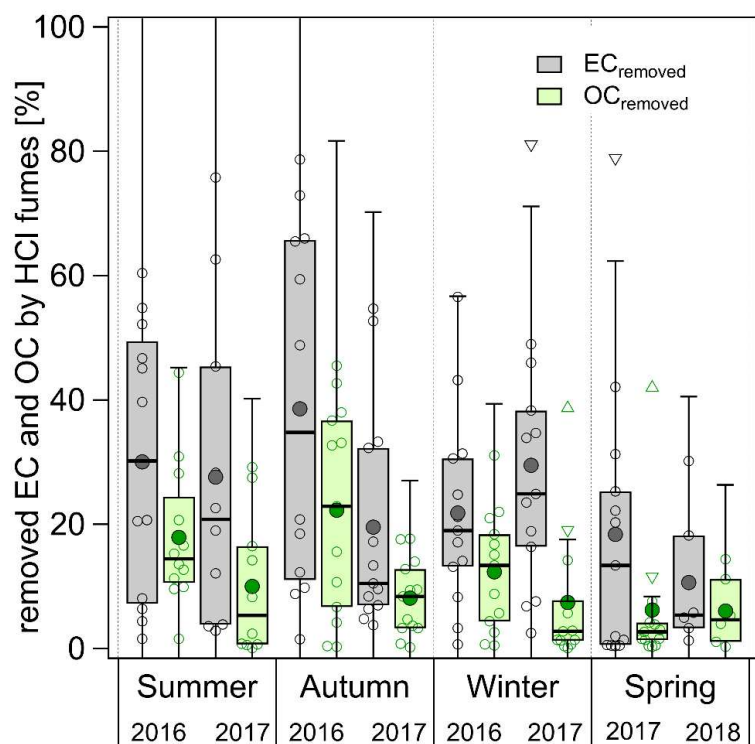


Figure S3. Seasonally differentiated percentage contributions of falsely determined OC and EC, i.e., removed part of original EC and OC from TC by HCl fumes. The boxes correspond to the interquartile range (IQR; 25 and 75 percentile) with median represented by the inner solid line. The whiskers correspond to inner fences range ($1.5 \cdot \text{IQR}$), triangles are outliers and mean is represented by large filled circle.

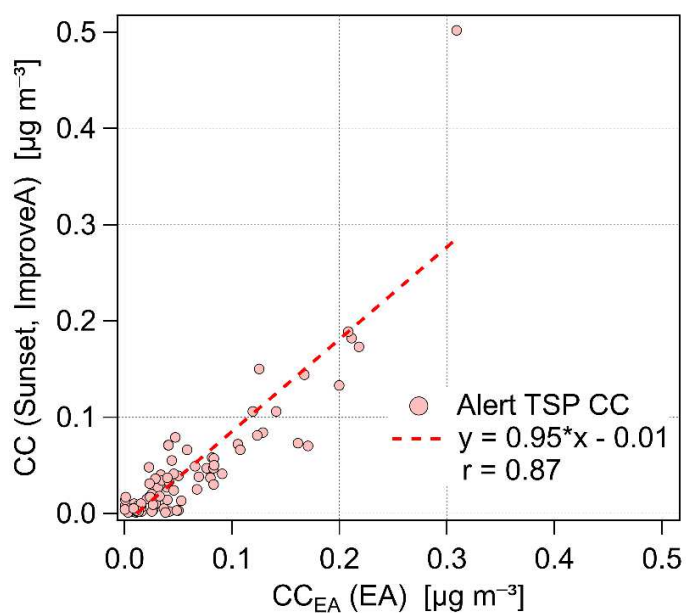


Figure S4. Comparison of CC concentrations calculated based on the EA and the EC/OC measurements.

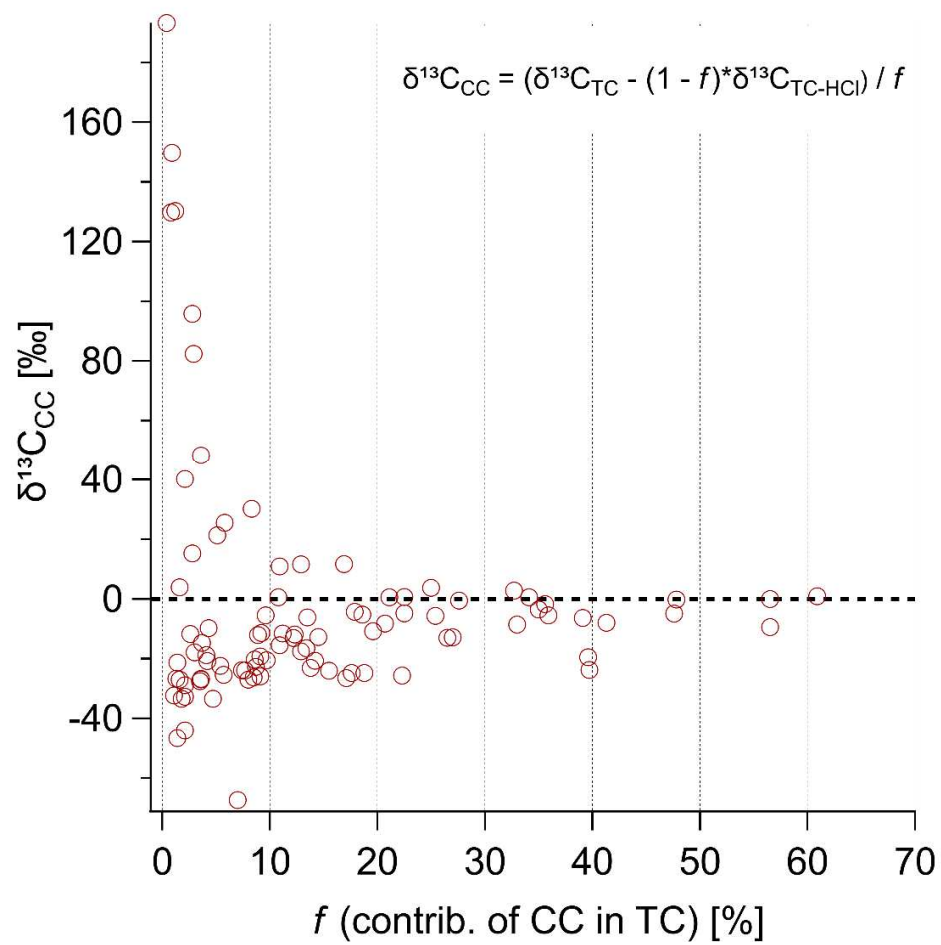


Figure S5. Relationship between calculated $\delta^{13}\text{C}_{\text{CC}}$ values and CC contribution in TC.

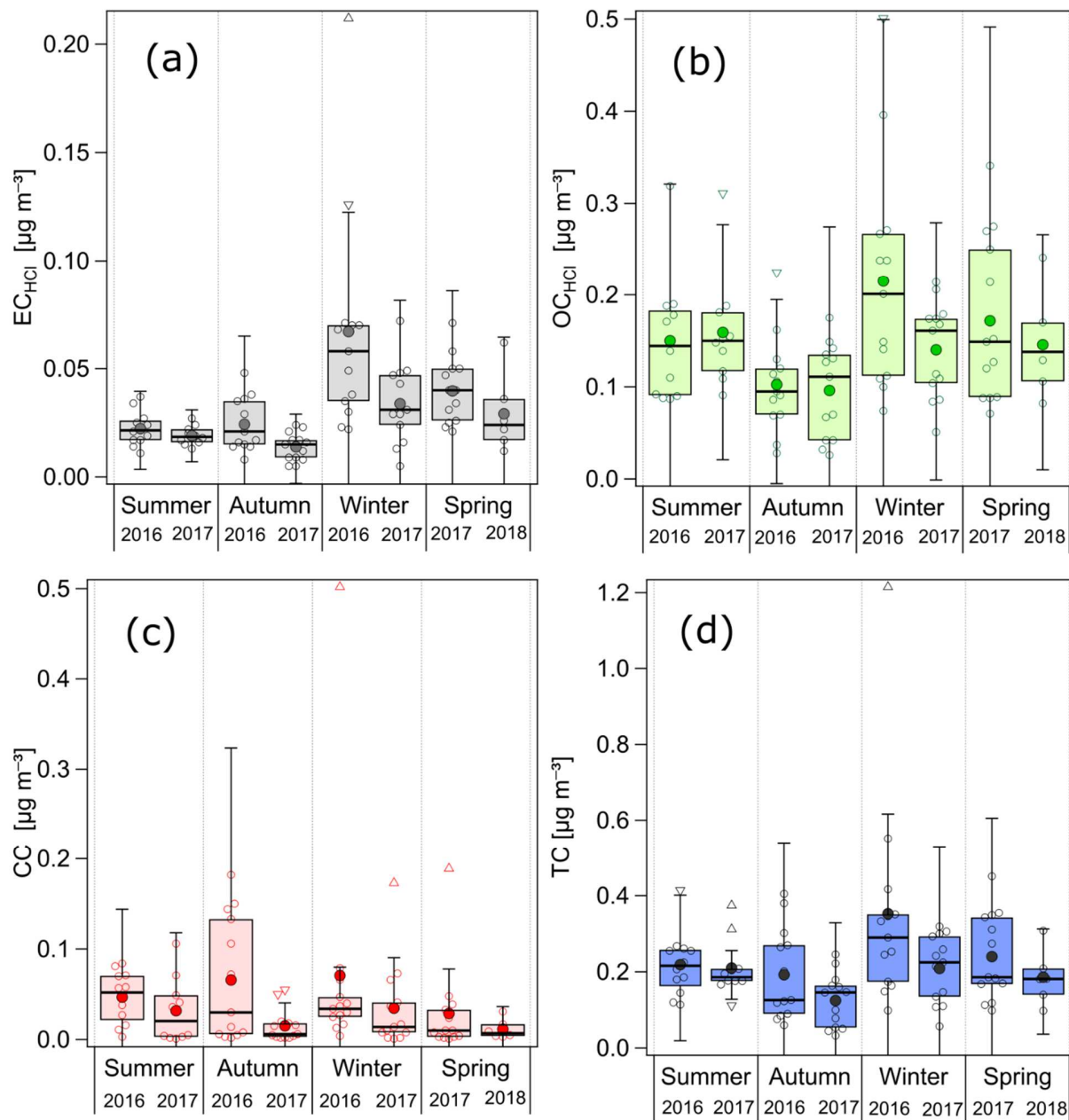


Figure S6. Seasonal variations of mass concentrations of (a) EC_{HCl} , (b) OC_{HCl} , (c) CC and (d) TC at Alert site. (TC = EC_{HCl} + OC_{HCl} + CC). The boxes correspond to the interquartile range (IQR; 25 and 75 percentile) with median represented by the inner solid line. The whiskers correspond to inner fences range ($1.5 \times IQR$), triangles are outliers and mean is represented by large filled circle.

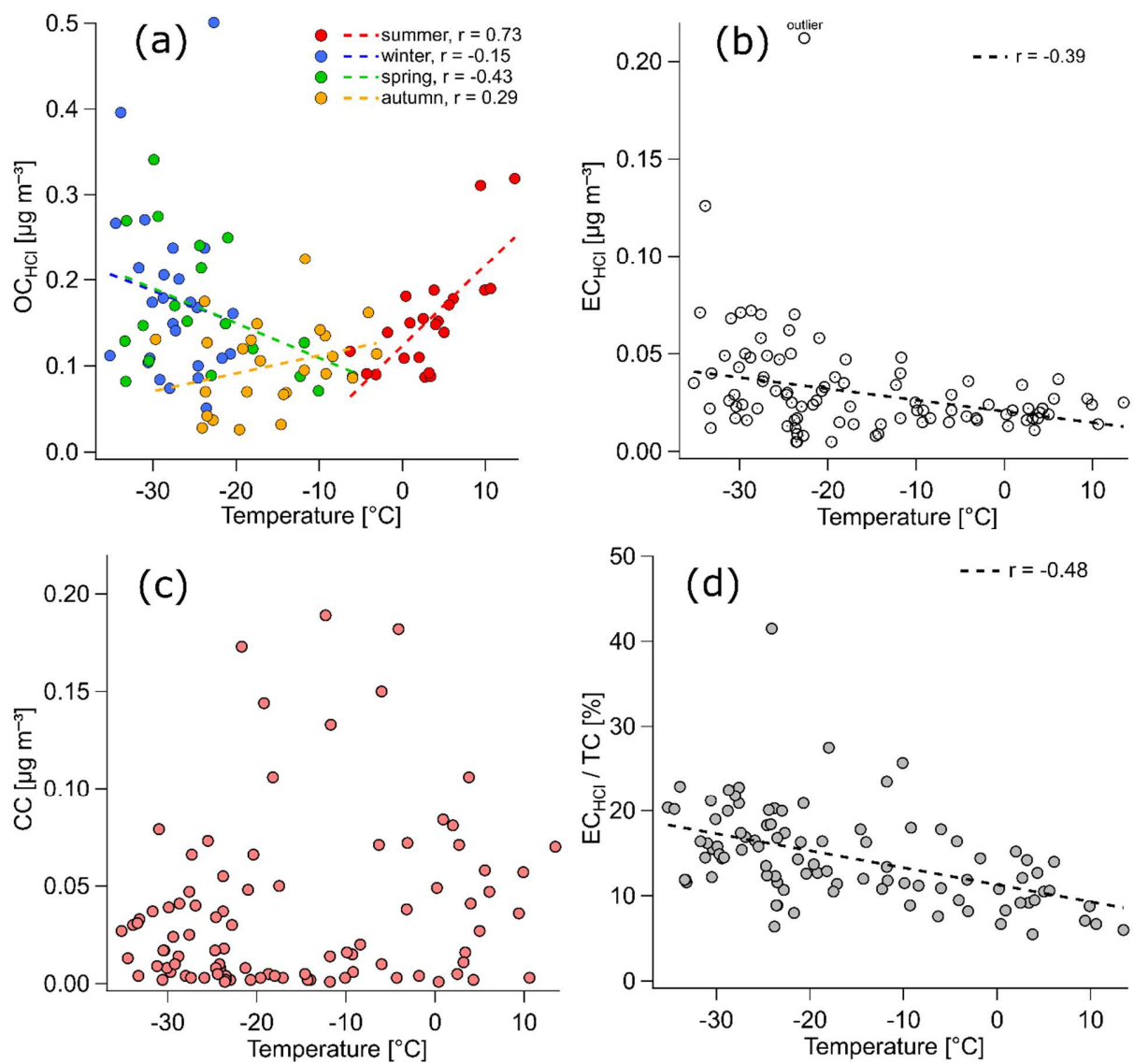


Figure S7. Changes in (a) OC_{HCl} , (b) EC_{HCl} and (c) CC mass concentrations, and (d) EC_{HCl}/TC ratio as a function of ambient temperature.

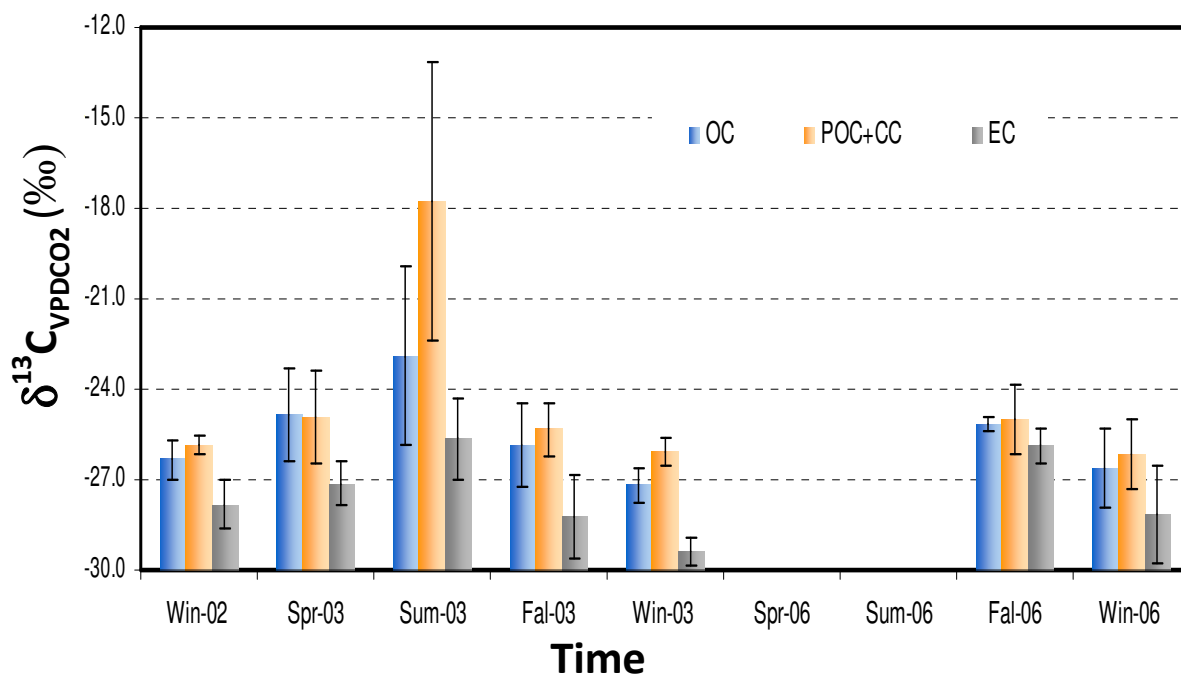


Figure S8. Seasonal variations of $\delta^{13}\text{C}$ in OC, pyrolytic carbon (POC) + CC, and EC in PM_{10} fine aerosol at the Alert station during 2002-2003 and 2006.

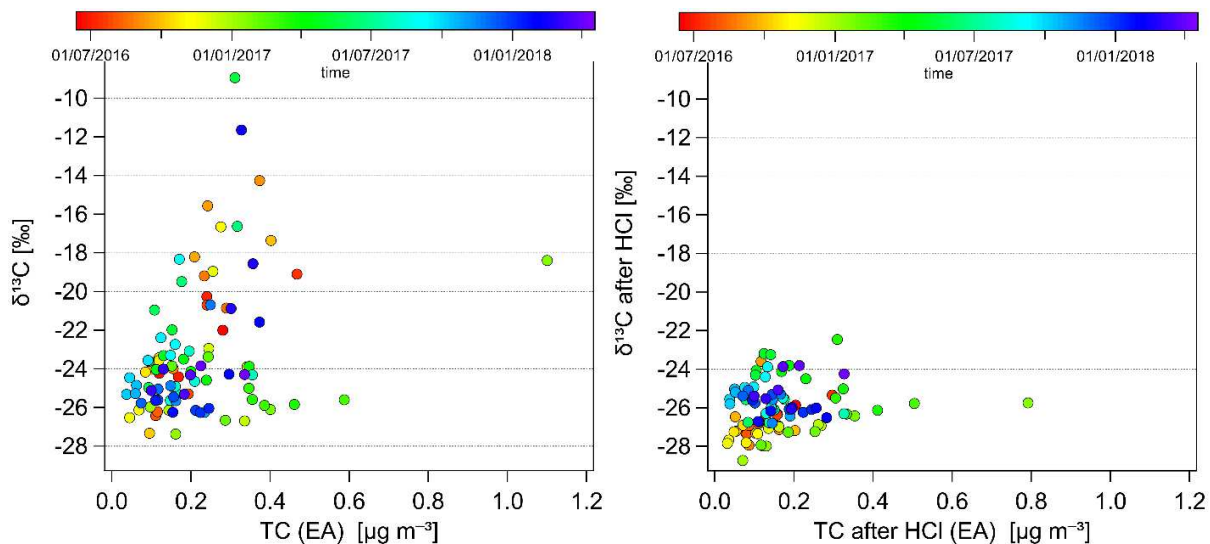


Figure S9. Relationship between $\delta^{13}\text{C}$ of TC and TC mass concentrations for untreated samples (left) and HCl treated samples (right). The color scale reflects the time of sample collection.

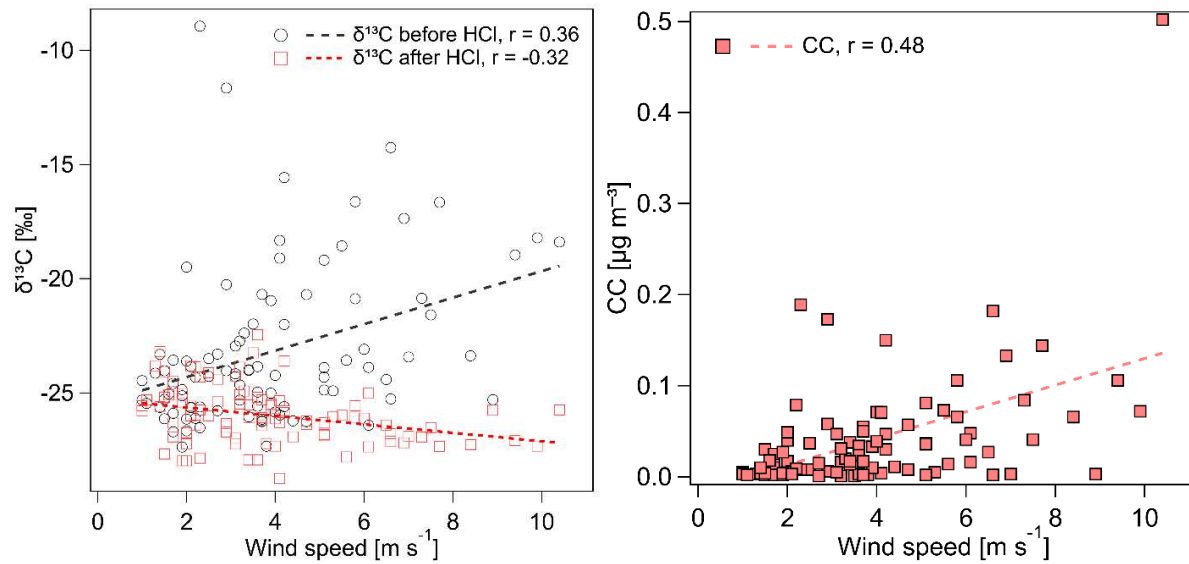


Figure S10. Dependence of $\delta^{13}\text{C}$ (right) and CC concentrations (left) on wind speed.

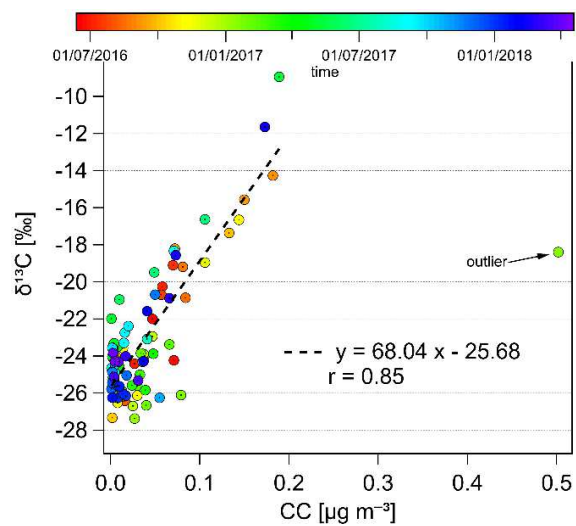


Figure S11. Dependence of $\delta^{13}\text{C}$ on CC concentration. The color scale reflects the time of sample collection.

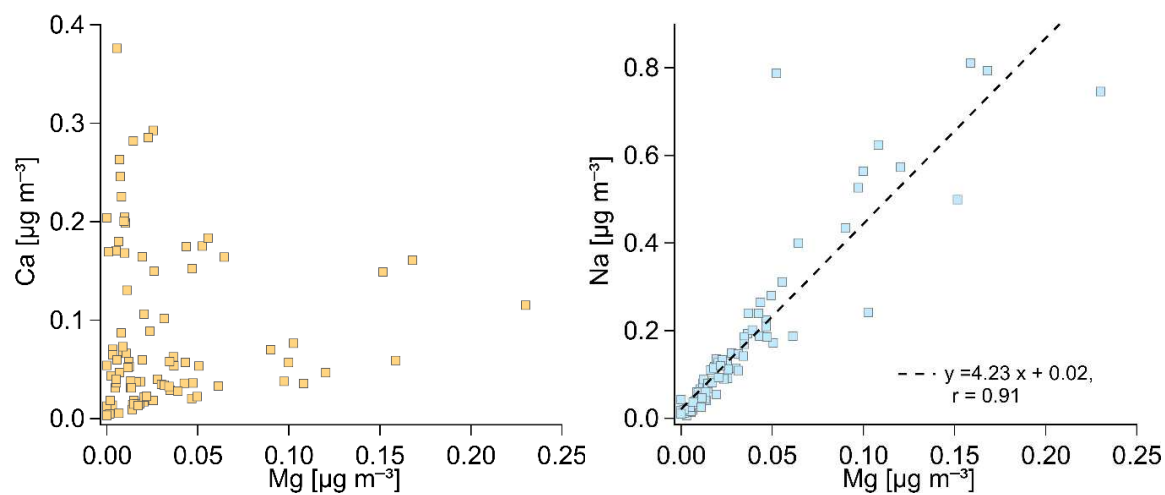


Figure S12. Relationship between Ca and Mg (right), and Na with Mg mass concentrations (left).